Comparison of the oxidation products produced by tetrahalobisphenol A flame retardants as a result of potassium monopersulfate oxidation with an iron(III)-tetrakis(*p*-sulfonatophenyl)porphyrin in the presence of humic acid

YUSUKE MIZUTANI, SHOHEI MAENO, QIANQIAN ZHU and MASAMI FUKUSHIMA*

Laboratory of Chemical Resources, Division of Sustainable Resources Engineering, Faculty of Engineering, Hokkaido University, Sapporo 060-8628, Japan

Short Heading: *TBBPA and TCBPA Oxidation by FeTPPS*

*Address correspondence to Masami Fukushima, Laboratory of Chemical Resources, Division of Sustainable Resources Engineering, Faculty of Engineering, Hokkaido University, Sapporo 060-8628, Japan; Phone: +81-11-706-6304, Fax: +81-11-706-6304;

E-mail: m-fukush@eng.hokudai.ac.jp

Received August 7, 2013

ABSTRACT

Tetrabromobisphenol A (TBBPA) and tetrachlorobisphenol A (TCBPA), commercially used halogenated flame retardants, can be found in leachates from landfills, because hydrophobic interactions with humic acids (HAs), major organic components in landfills, result in an increase in their solubility. The oxidation characteristics of TBBPA and TCBPA in the presence of HA were compared using a catalytic system comprised of a combination of iron(III)-tetrakis(*p*-sulfophenyl)porphyrin (FeTPPS) and $KHSO_5$ that can mimic the enzymatic reactions that occur in landfills. The levels of degradation and dehalogenation of TBBPA and TCBPA at pH 4 were significantly lower than at pH 8, which is a typical pH value for landfill leachates. In the presence of HA at pH 8, 2-hydroxyisopropyl-2,6 -dihalophenols (2HIP-26DXPs) were detected as major byproducts. These compounds are likely produced via the β-carbon scission of the substrates, and their levels decreased with increasing reaction time. The levels of coupling compounds between 2,6-dihalopnenols and TBBPA or TCBPA increased with reaction time. The 27% of Br in the degraded TBBPA and 50% of Cl in the degraded TCBPA were incorporated into the HA as a result of catalytic oxidation via the FeTPPS/$KHSO_5$ system. These results suggest that TCBPA is incorporated into HA more readily than TBBPA. The coupling compounds between HA and halogenated intermediates from TBBPA or TCBPA were assigned by pyrolysis-gas chromatography/mass spectrometry.

Keywords: Humic acid, tetrabromobisphenol A, tetrachlorobisphenol A, catalytic oxidation, oxidative coupling, iron(III)-5,10,15,20-tetrakis(*p*-sulfonatophenyl)porphyrin.

INTRODUCTION

Tetrabromobisphenol A (TBBPA) and tetrachlorobisphenol A (TCBPA), widely used halogenated flame retardants, can function as endocrine disruptors.[1,2] These compounds are mainly incorporated into epoxy and polycarbonate resins that are used in the manufacture of printed circuit boards for information technology and other electronic equipment.[3] TBBPA is a commonly used flame retardant, and the chloro analog TCBPA is also used as an additive to a lesser extent.[3] The leaching of such halogenated flame retardants from wastes derived from the above materials has been reported to be enhanced in the presence of humic acids (HAs) in landfills via hydrophobic interactions.[4,5] In general, the log K_{OW} values for brominated phenols (e.g., 5.3 for pentabromophenol[6]) are larger than those for chlorinated phenols (e.g., 4.08 for pentachlorophenol[7]). Thus, TBBPA (log K_{OW} 4.5 – 5.3[8]) may be more hydrophobic than TCBPA, while the log K_{OW} value for TCBPA has not been reported. Such differences between TBBPA and TCBPA are related to the degree of hydrophobic interaction with HAs, their mobility and ease of degradation in landfills.

HAs in landfills are mainly generated from organic wastes via microbial processes.[9,10] Oxidative

processes with peroxidase enzymes, as well as anaerobic fermentation accompanying by the generation of CH_4, play important roles in the genesis of HAs in landfills.[11-13] Peroxidases, classified as members of the cytochrome P-450 family, catalyze the demethylation of lignin and the hydroxylation and polymerization of phenols in organic wastes.[14] In addition, peroxidases catalyze the oxidation of chlorophenols and their oxidation intermediates are incorporated into polymeric structures in HAs via oxidation coupling.[15] Thus, the incorporation of chlorophenols into HAs can contribute to their immobilization in soils and ultimate detoxification.[14,15] Such reactions would be expected to occur in landfills, and these processes might lead to the immobilization and/or the detoxification of halogenated flame retardants, such as TBBPA and TCBPA.

On the other hand, it is well known that water-soluble iron(III)-porphyrins are capable of catalyzing the oxidation of chlorophenols,[16-25] and such structures can be regarded as a model of the active center in oxidative enzymes, such as ligninases and peroxidases.[26] There have been a few reports of the oxidation of bromophenols by the iron(III)-porphyrin catalysts.[27-29] However, in the oxidation of halogenated phenols, halogen atom substituents on the phenols affect the levels of dehalogenation via the nucleophilic substitution of H_2O to form quinones.[30] In the present study, to better understand the metabolic pathways related to halogenated flame retardants in landfills, the oxidation characteristics of TBBPA and TCBPA were compared in an iron(III)-porphyrin/$KHSO_5$ catalytic system in the presence of HA.

MATERIALS AND METHODS

Materials

The HA sample used in this study was obtained from Shinshinotsu peat soil, as described in a previous report.[31] The result of a elemental analysis for the prepared HA was as follows: C 54.5%, H 5.35%, N 2.17%, O 35.1%, S 0.66% and ash 2.22%. The FeTPPS was synthesized according to a previous report.[32] TBBPA and TCBPA (98% purity) were purchased from Tokyo Chemical Industries (Tokyo), and $KHSO_5$ was obtained as a triple salt, $2KHSO_5 \cdot KHSO_4 \cdot K_2SO_4$ (Merck, Darmstadt, Hessen, Germany).

The 2-hydroxyisopropyl-2,6-dibromophenol (2HIP-26DBP) standard, was synthesized, according to the method by Eriksson et al.[33] The mass spectral data for the silylated 2HIP-26DBP were as follows, m/z [rel. abundance, fragment ions]: 382 [3.4, M^+], 367 [17.2, $(M - CH_3)^+$], 364 [24.6, $(M - H_2O)^+$], 349 [62.0, $(M - (CH_3)(H_2O))^+$], 270 [30.8, $((CH_3)_2SiOC_3Br_2)^+$], 139 [26.2, $((CH_3)_2SiOC_5H_5)^+$]. For the synthesis of 2-hydroxyisopropyl-2,6-dichlorophenol (2HIP-26DCP), 4-isopropylphenol (0.5 mmole), anhydrous $FeCl_3$ (1 mmole) and *N*-chlorosuccinimide (1.25 mmole) were dissolved in 5 mL of acetonitrile. After stirring vigorously for 10 h at ambient temperature, 20 mL of $Na_2S_2O_3$ (10% aqueous) was added to quench the reaction. The resulting mixture was acidified by adding 10 mL of aqueous 1 M HCl, and the solution then extracted with ethyl acetate.

98 The yellowish extract was washed with aqueous 0.6 M HCl and then water. After dehydrating with
99 anhydrous Na_2SO_4, the solvent was removed by evaporation under reduced pressure. The obtained
100 residue was dissolved in CH_2Cl_2 and purified using a silica gel column with an eluent composed of
101 CH_2Cl_2/*n*-hexane (1/1, v/v). The obtained material was 4-isopropyl-2,6-dichlorophenol (yield 48%).
102 Mass spectral data for the silylated compound were as follows, m/z [rel. abundance, fragment ions]:
103 276 [16.4, M^+], 261 [59, $(M - CH_3)^+$], 183 [41.2, $(M - C_4H_7Cl)^+$]. The
104 4-isopropyl-2,6-dichlorophenol (0.24 mmole) was dissolved in 20 mL of CCl_4, and irradiated with
105 UV-light (254 nm) for 5 min. After stopping the irradiation, 100 μL of Br_2 in CCl_4 (626 mM) was
106 added to the mixture, and this solution was then irradiated for an additional 15 min. After standing
107 for 12 h under the dark at ambient temperature, the solvent was evaporated. The obtained residue
108 was dissolved in 200 mL of 0.025 M aqueous NaOH and the solution pH was adjusted to 9 by
109 adding HCl aqueous. After stirring for 3 days in the dark at ambient temperature, the solution was
110 acidified to pH 2 with aqueous HCl and the 2HIP-26DCP in the reaction mixture was extracted with
111 CH_2Cl_2. After removing the CH_2Cl_2 by evaporation, the residue was collected (yield 23%). Mass
112 spectral data for the silylated 2HIP-26DCP were as follows, m/z [rel. abundance, fragment ions]:
113 292 [6.08, M^+], 274 [33.7, $(M - H_2O)^+$], 259 [73.4, $(M - (H_2O)CH_3)^+$], 219 [11.4, $(M - (CH_3)_3Si)^+$],
114 183 [54.4, $(M - (CH_3)_3Si(HCl))^+$].
115

Test for TBBPA and TCBPA Degradations

A 2 mL aliquot of 0.02 M citrate/phosphate buffer, containing 50 μM TBBPA or TCBPA, 0 or 50 mg L^{-1} HA and 0.05 – 5 μM FeTPPS at pH 4 or 8, was placed in a 20-mL L-shaped glass tube. Subsequently, 25 μL of 0.01 M aqueous potassium monopersulfate ($KHSO_5$) was added, and the tube was then subjected to shaking at 25 ^oC in an incubator. After the reaction, 1 mL of 2-propanol was added to the reaction mixture and a 20-μL aliquot of the resulting solution was injected into a PU-980 type HPLC pumping system (Japan Spectroscopic Co.). The mobile phase consisted of a mixture of 0.08% aqueous H_3PO_4 and methanol (22/78 for TBBPA, 25/75 for TCBPA, v/v), and the flow rate was set at 1 mL min^{-1}. A 5C18-MS Cosmosil packed column (4.6 mm id × 250 mm, Nacalai Tesque) was used as the solid phase, and the column temperature was maintained at 50 °C. The UV absorption of TBBPA or TCBPA was measured at 220 nm. Bromide or chloride ions in the reaction mixture were analyzed by an ion chromatography.

Analysis of Oxidation Intermediates

The catalytic oxidation system, described above, was scaled up to 25 mL at pH 8. After reaction periods of 1-, 5-, 10- or 30-min, 1 mL of aqueous, 1 M ascorbic acid was added, and the pH of the solution was adjusted to 11–11.5 by adding aqueous K_2CO_3 (600 g L^{-1}). Subsequently, 5 mL of acetic anhydride was added dropwise to the solution, and 0.5 mL of a 1 mM anthracene solution in

hexane/acetone mixture (1/1, v/v) was added as an internal standard (ISTD) for the GC/MS analysis. This mixture was doubly extracted with 15 mL of *n*-hexane, and the extract was then dried over anhydrous Na_2SO_4. After filtration, the extract was evaporated under a stream of dry N_2, and the residue was dissolved in 0.25 mL of *n*-hexane. A 1 μL aliquot of the extract was introduced into a GC-17A/QP5050 GC/MS system (Shimadzu, Kyoto). A Quadrex methyl silicon capillary column (0.25 mm id × 25 m) was employed in the separation. The temperature ramp was as follows: 65 °C for 1.5 min, 65–120 °C at 35 °C min^{-1}, 120–300 °C at 4 °C min^{-1} and a 300 °C held for 10 min.

Separation and Analysis of HA Fraction

The oxidation of TBBPA or TCBPA in the presence of HA was conducted at pH 4 and 8, resulting in the incorporation of brominated or chlorinated intermediates into the HA. The volume of the initial buffer solution was scaled up to 200 mL. In this experiment, the concentrations of HA and TBBPA or TCBPA were fixed at 100 mg L^{-1} and 100 μM, respectively. The concentrations of TBBPA or TCBPA in the reaction mixtures before and after the oxidation were determined by HPLC. After a 30-min period, 2 mL of 1 M ascorbic acid and 100 mL of 2-propanol were added to the reaction mixture. The HA fraction was then concentrated and deionized by ultrafiltration through a Millipore YM1 ultrafiltration cellulose membrane (molecular weight cut-off of 1 kDa). In the ultrafiltration system, the concentrated HA fraction was washed twice with 100 mL of pure

water. The resulting HA fraction was further purified by dialysis against pure water using a Spectra/Por cellulose ester membrane (1 kDa). The HA fraction was then obtained in powdered form by freeze-drying. The prepared samples were analyzed by pyrolysis-gas chromatography/mass spectrometry with online methylation using tetramethylammonium hydroxide (TMAH-py-GC/MS). A 1.0 ± 0.1 mg portion of the powdered sample was placed in a 50 μL deactivated stainless steel cup. A 25 μL aliquot of tetramethylammonium hydroxide in methanol (40 mg mL^{-1}) were then added to the cup, and the solvent was removed under reduced pressure. After repeating this procedure 4 times, the cup was introduced into a PY-2020D type Pyrolyzer (Frontier Laboratories Ltd., Koriyama, Fukushima) connected to a Shimadzu GC-17A/QP5050 type GC/MS system. Helium (99.995 % purity) was used as the carrier gas, and flash pyrolysis of the powdered samples were carried out at 550 °C for 0.4 min. A Quadrex 100 % dimethylpolysiloxane capillary column (0.25 mm i.d. × 25 m, 0.25 μm film thickness) was employed in the separation of the pyrolysate compounds. The temperature program for the GC oven was as follows: 50 °C for 1 min; 50 – 300 °C at a heating rate of 5 °C min^{-1}; 300 °C for 4 min.

RESULTS AND DISCUSSION

Evaluation of Turnover Number

Figures 1 and 2 provide information on the influence of the [FeTPPS] on the concentrations of

degraded TBBPA or TCBPA (Δ[TBBPA] or Δ[TCBPA]) and on the [Br^-] or [Cl^-] that are released during the oxidation. The degradation and dehalogenation of TBBPA and TCBPA increased with increasing [FeTPPS] at pH 4, while reached a plateau at pH 8 above 0.5 μM of [FeTPPS]. The levels of degradation and debromination at pH 8 were significantly higher than the corresponding values at pH 4. The presence of HA resulted in decrease in the degradation and debromination of TBBPA at pH 4.

The efficiencies of TBBPA and TCBPA degradation should be precisely evaluated in terms of moles of degraded substrate per mole of catalyst per minute, that is, as the turnover frequency for the catalyst. However, TBBPA and TCBPA were degraded within 1 min and after this period, a plateau was reached at pH 4 and 8 in the FeTPPS/$KHSO_5$ catalytic system. Thus, it was not possible to evaluate the kinetics of degradation and dehalogenation from the present data. Alternatively, the efficiency of degradation for TBBPA or TCBPA was evaluated as mole of degraded substrate per mole of catalyst, that is, the turnover number (TON). The TON values were estimated by dividing Δ[TBBPA] or Δ[TCBPA] by [FeTPPS] (Table 1). At pH 4, the TONs for degradation and dehalogenation of TCBPA were significantly higher than those for TBBPA. Such trends are consistent with the levels of degradation and dehalogenation for 2,4,6-trihalophenols in the presence of water-soluble iron(III)-porphyrin catalysts at pH 3 in a previous report and are reported to be dependent on the electronegativity of substituents on the aromatic carbons.[30] Although the TON

188 values at pH 8 were much larger than those at pH 4, the presence of HA resulted in a decrease in
189 TONs for the degradation and dehalogenation of TBBPA and TCBPA. At pH 4, the majority of
190 acidic functional in HA are protonated species,[36] and HAs can exist as colloidal forms.[35] In
191 contrast, acidic functional groups in HAs are almost dissociated at pH 8, and HAs can exist as ionic
192 forms with the large negative electrostatic field.[34] It has been reported that the lower levels of
193 carboxylic groups in HAs result in the higher adsorption of hydrophobic organic pollutants, such as
194 chlorinated dioxin.[36] This suggests that the lower levels of the degradation and dehalogenation in
195 the presence of HA at pH 4 can be attributed to the adsorption of TBBPA or TCBPA to the HA.
196 Thus, a higher pH value appears to be preferable for the catalytic oxidation of TBBPA and TCBPA
197 using the FeTPPS/$KHSO_5$ system, while the presence of HA inhibits the reactions.
198
199 **Oxidation Products**
200 The average pH for landfill leachates is reported to be 8.53.[4,5] Because TBBPA and TCBPA (pK_a
201 7.5 – 7.6) exist as phenolate anions under such weak alkaline conditions, the mobility of these
202 compounds may be enhanced. In addition, landfill leachates contains several-ten mg L^{-1} of HAs as
203 dissolved organic carbon, and these also facilitate the mobility of TBBPA and TCPBA.[4,5] Thus, the
204 oxidation characteristics of TBBPA and TCBPA in the presence of the FeTPPS/$KHSO_5$ system at
205 pH 8 in the presence of HA should be the focus of scientific attention, in terms of their fates in

206 landfills. To identify the oxidation products produced in the reactions, *n*-hexane extracts of
207 acetylated reaction mixtures were analyzed by GC/MS after for a variety of reaction periods (1 – 30
208 min). Chromatograms of these mixtures are shown in Fig. 3. After a reaction period of 1 min, peaks
209 at 17.8 min (Fig. 3a, ▼) and 13.6 min (Fig. 3b, ◊) were detected as major oxidation products. These
210 peaks were assigned as 2HIP-26DBP and 2HIP-26DCP based on mass spectral data (Fig. 4a and c).
211 However, these peaks were largely decreased after a reaction period of 30 min, while a series of new,
212 small peaks appeared at 56.0 min (Fig. 3a, ●) and 52.6 min (Fig. 3b, ○). As shown in Fig. 4b and d,
213 these peaks were assigned as acetates of coupling compounds produced by reactions between
214 TBBPA or TCBPA and 2,6-dibromophenol (26DBP) or a 2,6-dichlorophenol (26DCP) intermediate.
215 Figure 5a provides information on the kinetics of formation of 2HIP-26DBP and 2HIP-26DCP.
216 The percent conversion of TBBPA or TCBPA to 2HIP-26DBP or 2HIP-26DCP was estimated by
217 dividing the molar concentrations of the products by that for the degraded substrates. 70% of
218 TBBPA and 83% of TCBPA were initially converted into 2HIP-26DBP and 2HIP-26DCP,
219 respectively, while the percent conversion decreased after a reaction time of 1 min. Figure 5b shows
220 the kinetics of formation of coupling compounds between TBBPA or TCBPA and 26DBP or the
221 26DCP intermediate. The peak areas (ratio of the peak areas for the product to ISTD) increase with
222 increasing reaction time. It has been reported that oxidation of TBBPA by δ-MnO_2 or UV-light
223 irradiation leads to β-carbon scission, with the formation of 2,6-dibromo-*p*-benzoquinone as well as

2HIP-26DBP.[33,37] Although 2,6-dibromo-*p*-benzoquinone could be extracted with *n*-hexane after reduction to 2,6-dibromo-*p*-hydroquinone followed by acetylation,[27,28] this type of compound was not detected in *n*-hexane extracts of reaction mixtures as a result of the catalytic oxidation of TBBPA or TCBPA on the FeTPPS/$KHSO_5$ system. Although 2HIP-26DBP and 2HIP-26DCP were detected as major products that were produced via β-carbon scission, it is possible that the remaining 26DBP or 26DCP could be present as radical species. Thus, the production of coupling compounds between TBBPA or TCBPA and 26DBP or the 26DCP intermediate can be attributed to coupling between phenoxy radicals derived from TBBPA or TCBPA and radical species derived from the scission of the β-carbons in TBBPA and TCBPA.

Halogenated Intermediates in Humic Acid Fractions

It has been reported that halogenated intermediates that are produced as a result of the oxidation of halogenated phenols by the iron(III)-porphyrin catalyst in the presence of HAs can be incorporated into HAs via covalent binding.[22,29] Thus, the majority of halogenated intermediates from the oxidation of TBBPA and TCBPA may be incorporated into the HA. To characterize the halogenated intermediates that are incorporated into HA as a result of catalytic oxidation via the FeTPPS/$KHSO_5$ catalytic system, TBBPA or TCBPA were oxidized in the presence of HA (initial substrate concentration 100 μM, HA concentration 100 mg L^{-1}), and the HA fractions were then separated. In

242 this experiment, changes in Δ[TBBPA] and Δ[TCBPA] were monitored by HPLC: 87 μM for
243 TBBPA; 95 μM for TCBPA. The Br and Cl contents in the powdered samples of the HA fractions
244 after reaction with TBBPA and TCBPA (*W*) were determined: 7.5% for Br; 6.7% for Cl. Based on
245 these results, the percent conversion of tetrahalobisphenol A (TXBPA) to halogenated intermediates
246 incorporated into HA (*A*) can be calculated as:

247 $$A\ (\%) = \frac{\frac{W\ (\%)}{100} \times 0.2\ (\mathrm{L}) \times [\mathrm{HA}](\mathrm{g\ L^{-1}})}{\Delta[\mathrm{TXBPA}]\ (\mathrm{M}) \times 0.2(\mathrm{L}) \times 4 \times (\text{atomic weight of Br or Cl})} \times 100$$

248 The *A* values were estimated to be 27% for TBBPA and 50% for TCBPA. These results indicate that
249 the level of the incorporation of halogenated intermediates into HA for TCBPA is higher than that
250 for TBBPA.

251 To identify the halogenated intermediates in the HA fractions after oxidation with TBBPA or
252 TCBPA, powdered samples were analyzed by TMAH-py-GC/MS. Figure 6A shows pyrograms for
253 the HA fractions after reaction with TBBPA (i) and TCBPA (ii). The peak number indicates the
254 pyrolysate compounds derived from the pyrolysis of HA and the assignment for these peaks are
255 shown in Fig. 6B, based on the NIST mass spectral library and previous reports on
256 TMAH-py-GC/MS of HAs.[38,39] The peaks shown by alphabetical symbols (*a* – *h*) were
257 halogenated pyrolysate compounds related to intermediates from the oxidation of TBBPA and
258 TCBPA. The expected structures were identified based on interpretations of fragment ions from
259 mass spectral data for each pyrolysate compound. The identified fragment ions and predicted

structures are summarized in Table 2. These results clearly demonstrate that halogenated intermediates are incorporated into HA via covalent binding as a result of TBBPA or TCBPA oxidation in the presence of the FeTPPS/$KHSO_5$ catalytic system. Although the brominated intermediates from TBBPA were mainly 2,6-dibromophenol derivatives, a monochloro intermediate (peak *f* in Table 2) was found in the pyrolysate compounds for TCBPA, which is consistent with the result showing that the levels of dechlorination are higher than the corresponding values for debromination. The largest peaks of halogenated intermediates in pyrograms (i) and (ii) in Fig. 6A were peaks *c* and *g*, respectively. These components were structurally similar to the substrates, TBBPA (peak *c*) and TCBPA (peak *g*). The formation of such pyrolysate compounds suggest the coupling of phenoxy radicals from TBBPA or TCBPA with HA.

Based on the results described above and the known reactivity of FeTPPS activated by $KHSO_5$,[26] possible tetrahalobisphenol A (TXBPA) oxidation pathways in the presence of HAs can now be proposed (Fig. 7). Initially, $KHSO_5$ reacts with Fe^{III}TPPS in the catalyst to generate high-valent iron-oxo porphyrin cation radicals ($O=Fe^{IV}TPPS^{+\bullet}$). This active species reacts with TXBPA to give an iron-oxo species ($O=Fe^{IV}$TPPS) and a phenoxy radical species ($TXBPA^{\bullet}$). Similarly, phenolic moieties in HA can be oxidized to give phenoxy radicals in the presence of the FeTPPS/$KHSO_5$ catalytic system. The β-carbon scission of $TXBPA^{\bullet}$ leads to the production of the 2,6-dihalophenoxy radical ($26DXP^{\bullet}$) and 4-isopropylene -2,6-dihalophenone (4IP-26DXP).[37]

2,6-Dihalobenzo-*p*-quinone was not detected as an oxidation product in the present study, suggesting that 26DXP$^{\bullet}$ couples instantaneously with radical species of HA or other radical species to yield further polymerized compounds. On the other hand, the further oxidation of 4IP-26DXP by active species of FeTPPS results in the formation of a 4-isopropyl-2,6-dihalophenolate cation (4IP-26DXP^{+}), and the nucleophilic addition of H_2O to 4IP-26DXP^{+} results in the formation of 2HIP-26DXP. The findings herein indicate that 2HIP-26DXP is formed at the initial stage of the oxidation and its concentration then decreases. Thus, radical species of 2HIP-26DXP (2HIP-26DXP$^{\bullet}$), which are formed by the active species of FeTPPS, can be covalently incorporated into HA via radical coupling reactions.

CONCLUSION

TBBPA and TCBPA were effectively oxidized in the presence of HA at pH 8, which corresponds to the pH values typically found in landfill leachates. Although the levels of dechlorination were significantly higher than those for debromination, the oxidation characteristics of TXBPAs were similar, in terms of oxidation products. 2HIP-26DXPs were detected as major byproducts as a result of the β-carbon scission of substrates in the initial stages of the reaction, and levels of these decreased with increasing reaction time. The halogenated intermediates were incorporated into HA as a result of catalytic oxidation. The content of Br incorporated into HA (27%) was smaller than

296 that for Cl (50%). These results suggest that TCBPA is incorporated into HA more easily than
297 TBBPA as the result of oxidation reactions in landfills by oxidative enzymes that can be mimicked
298 by the FeTPPS/$KHSO_5$ catalytic system.
299
300 **ACKNOWLEDGMENTS**
301 This work was supported by Grants-in-Aid for Scientific Research of the Japan Society for the
302 Promotion of Science (25241017).
303
304 **REFERENCES**
305 [1] Kitamura, S.; Suzuki, T.; Sanoh, S.; Kohta, R.; Jinno, N.; Sugihara, K.; Yoshihara, S.-i.;
306 Fujimoto, N.; Watanabe, H.; Ohta, S. Comparative study of the endocrine-disrupting activity of
307 bisphenol A and 19 related compounds. Toxicol. Sci. **2005**, *84*, 249-259.
308 [2] Kitamura, S.; Jinno, N.; Ohta, S.; Kuroki, H.; Fujimoto, N. Thyroid hormonal activity of the
309 flame retardants tetrabromobisphenol A and tetrachlorobisphenol A. Biochem. Bioph. Res. Co. 2002,
310 293, 554-559.
311 [3] van Esch, G.J. *Flame retardants: A General Introduction*, Environmental Health Criteria 192;
312 World Health Organization: Geneva, Switzerland, 1997; pp.61-121.
313 [4] Osako, M.; Kim, Y.-J.; Sakai, S. Leaching of brominated flame retardants in leachate from land

314 hills in Japan. Chemosphere **2004**, *57*, 1571-1579.

315 [5] Choi, K.-I.; Lee, S.-H.; Osako, M. Leaching of brominated flame retardants from TV housing

316 plastics in the presence of dissolved humic matter. Chemosphere **2009**, *74*, 460-466.

317 [6] Kuramochi, H.; Maeda, K.; Kawamoto, K., Water solubility and partitioning behavior of

318 brominated phenols. Environ. Toxicol. Chem. **2004**, *23*, 1386-1393.

319 [7] Nowoseielski, B.E.; Fein, J.B., Experimental study of octanol-water partition coefficients for

320 2,4,6-trichlorophenol and pentachlorophenol: Derivation of an empirical model of chlorophenol

321 partitioning behavior. Appl. Geochem. **1998**, *13*, 893-904.

322 [8] Salapasidou, M.; Samara, C.; Voutsa, D. Endocrine disrupting compounds in the atmosphere of

323 the urban area of Thessaloniki, Greece. Atmos. Environ. **2011**, *45*, 3720-3729.

324 [9] Xiaoli, C.; Shimaoka, T.; Qiang, G.; Youcai, Z. Characterization of humic and fulvic acids

325 extracted from landfill by elemental composition, ^{13}C CP/MAS NMR and TMAH-Py-GC/MS.

326 Waste Manage. **2008**, *28*, 896-903.

327 [10] He, X.-S.; Xi, B.-D.; Wei, Z.-M.; Jiang, Y.-H.; Geng, C.-M.; Yang, Y.; Yuan, Y.; Liu, H.-L.

328 Physicochemical and spectroscopic characteristics of dissolved organic matter extracted from

329 municipal solid waste (MSW) and their influence on the landfill biological stability. Bioresource

330 Technol. **2011**, *102*, 2322-2327.

331 [11] Jayasinghe, P.A.; Hettiaratchi, J.P.A.; Mehrotra, A.K.; Kumar, S. Effect of enzyme additions on

methane production and lignin degradation of landfill sample of municipal solid waste. Bioresource Technol. **2011**, *102*, 4633-4637.

[12] Montgomery, R. Development of biobased products. Bioresource Technol. **2004**, *91*, 1-29.

[13] Kallistova, A.Y.; Kevbrina, M.V.; Nekrasova, V.K.; Shnyrev, N.A.; Einola, J.-K.M.; Kulomaa, M.S.; Rintala, J.A.; Nozhevnikova, A.N. Enumeration of methanotrophic bacteria in the cover soil of an aged municipal landfill. Microb. Ecol. **2007**, *54*, 637-645.

[14] Bollag, J.-M. Decontaminating soil with enzymes. Environ. Sci. Technol. **1992**, *26*, 1876-1881.

[15] Hatcher, P.G.; Bortiatynski, J.M.; Minard, R.D.; Dec, J.; Bollag, J.-M. Use of high-resolution ^{13}C NMR to examine the enzymatic covalent binding ^{13}C-labeled 2,4-dichlorophenol to humic substances. Environ. Sci. Technol. **1993**, *27*, 2098-2103.

[16] Shukla, R.S.; Robert, A.; Meunier, B., Kinetic investigations of oxidative degradation of aromatic pollutant 2,4,6-trichlorophenol by an iron-porphyrin complex, a model of ligninase. J. Mol. Catal. A-Chem. **1996**, *113*, 45-49.

[17] Fukushima, M.; Tatsumi, K., Effect of hydroxypropyl-β-cyclodextrin on the degradation of pentachlorophenol by potassium monopersulfate catalyzed with iron(III)-porphyrin complex. Environ. Sci. Technol. **2005**, *39*, 9337-9342.

[18] Fukushima, M.; Shigematsu, S.; Nagao, S., Degradation of pentachlorophenol in a contaminated soil suspension using hybrid catalysts prepared via urea-formaldehyde

polycondensation between tetrakis(hydroxyphenyl)porphineiron(III) and humic acid. Environ. Chem. Lett. **2011**, *9*, 223-228.

[19] Rismayani, R.; Fukushima, M.; Sawada, A.; Ichikawa, H.; Tatsumi, K., Effects of peat humic acids on the catalytic oxidation of pentachlorophenol using metalloporphyrins and metallophthalocyanines. J. Mol. Catal. A-Chem. **2004**, *217*, 13-19.

[20] Fukushima, M.; Sawada, A.; Kawasaki, M.; Ichikawa, H.; Morimoto, K.; Tatsumi, K.; Aoyama, M., Influence of humic substances on the removal of pentachlorophenol by a biomimetic catalytic system with a water-soluble iron(III)-porphyrin complex. Environ. Sci. Technol. **2003**, *37*, 1031-1036.

[21] Fukushima, M.; Shigematsu, S.; Nagao, S., Oxidative degradation of 2,4,6-trichlorophenol and pentachlorophenol in contaminated soil suspension using a supramolecular catalyst prepared via formaldehyde polycondensation between tetrakis(hydroxyphenyl)porphineiron(III) and humic acid. J. Environ. Sci. Heal. A **2009**, *44*, 1088-1097.

[22] Fukushima, M.; Ichikawa, H.; Kawasaki, M.; Sawada, A.; Morimoto, K.; Tatsumi, K., Effects of humic substances on the pattern of oxidation products of pentachlorophenol induced by a biomimetic catalytic system using tetra(*p*-sulfophenyl)porphineiron(III) and $KHSO_5$, Environ. Sci. Technol. **2003**, *37*, 386-394.

[23] Fukushima, M.; Shigematsu, S.; Nagao, S. Influence of humic acid type on the oxidation

368 products of pentachlorophenol using hybrid catalysts prepared by introducing
369 iron(III)-5,10,15,20-tetrakis(*p*-hydroxyphenyl)porphyrin into hydroquinone-derived humic acids.
370 Chemosphere **2010**, *78*, 1155-1159.
371 [24] Fukushima, M.; Shigematsu, S. Introduction of 5,10,15,20-tetrakis(4-hydroxyphenyl)
372 porphineiron(III) into humic acid via formaldehyde polycondensation. J. Mol. Catal. A-Chem. **2008**,
373 *293*, 103-109.
374 [25] Fukushima, M.; Tanabe, Y.; Morimoto, K.; Tatsumi, K. Role of humic acid fraction with higher
375 aromaticity in enhancing the activity of a biomimetic catalyst, tetra(*p*-sulfonatophenyl)
376 porphineiron(III). Biomacromolecules **2007**, *8*, 386-391.
377 [26] Sheldon, R.A. Oxidation catalysis by metalloporphyrins. *Metalloporphyrins in Catalytic*
378 *Oxidations*; Sheldon, R.A. Ed.; Dekker: New York, 1994; pp. 2-13.
379 [27] Shigetatsu, S.; Fukushima, M.; Nagao, S., Oxidative degradation of 2,6-dibromophenol using
380 an anion-exchange resin supported supramolecular catalysts of iron(III)-5,10,15,20-tetrakis
381 (*p*-hydroxyphenyl)porphyrin bound to humic acid prepared via formaldehyde and
382 urea-formaldehyde polycondensation. J. Environ. Sci. Heal. A **2010**, *45*, 1536–1542.
383 [28] Zhu, Q.; Mizutani, Y.; Maeno, S.; Nishimoto, R.; Miyamoto, T.; Fukushima, M. Potassium
384 monopersulfate oxidation of 2,4,6-tribromophenol catalyzed by a SiO_2-supported
385 iron(III)-5,10,15,20-tetrakis-(4-carboxyphenyl)porphyrin. J. Environ. Sci. Heal. A *in press*.

386 [29] Fukushima, M.; Ishida, Y.; Shigematsu, S.; Kuramitz, H.; Nagao, S. Pattern of oxidation
387 products derived from tetrabromobisphenol A in catalytic system comprised of iron(III)-tetrakis
388 (*p*-sulfophenyl)porphyrin, $KHSO_5$ and humic acids. Chemosphere **2010**, *80*, 860-865.
389 [30] Fukushima, M.; Mizutani, M.; Maeno, M.; Zhu, Q.; Kuramitz, H.; Nagao, S., Influence of
390 halogen substituents on the catalytic oxidation of 2,4,6-halogenated phenols by
391 Fe(III)-tetrakis(*p*-hydroxyphenyl) porphyrins and potassium monopersulfate. Molecules **2012**, *17*,
392 48-60.
393 [31] Fukushima, M.; Tanaka, S.; Nakayasu, K.; Sasaki, K.; Tatsumi, K. Evaluation of copper(II)
394 binding abilities of humic substances by a continuous site distribution model considering proton
395 competition. Anal. Sci. **1999**, *5*, 185-188.
396 [32] Kawasaki, M.; Kuriss, A.; Fukushima, M.; Sawada, A.; Tatsumi, K. Effects of pH and organic
397 co-solvents on the oxidation of naphthalene with peroxosulfate catalyzed by iron(III)
398 tetrakis(*p*-sulfonatophenyl)porphyrin. J. Porphyr. Phthalocya. **2003**, *7*, 645-650.
399 [33] Eriksson, J.; Rahm, S.; Green, N.; Bergman, Å.; Jakobsson, E. Photochemical transformations
400 of tetrabromobisphenol A and related phenols in water. Chemosphere **2004**, *54*, 117-126.
401 [34] Fukushima, M.; Tanaka, S.; Hasebe, K.; Taga, M.; Nakamura, H. Interpretation of acid-base
402 equilibrium of humic acid by continuous p*K* distribution model and electrostatic model. Anal. Chim.
403 Acta **1995**, *302*, 365-373.

404 [35] Terashima, M.; Fukushima, M.; Tanaka, S. Influences of pH on surface activity of humic acid:
405 micelle-like aggregate formation and interfacial adsorption. Colloid Surface A **2004**, *247*, 77-83.
406 [36] Tanaka, F.; Fukushima, M.; Kikuchi, A.; Yabuta, H.; Ichikawa, H.; Tatsumi, K. Influence of
407 chemical characteristics of humic substances on the partition coefficient of a chlorinated dioxin.
408 Chemosphere **2005**, *57*, 1319-1326.
409 [37] Lin, K.; Liu, W.; Gan, J. Reaction of tetrabromobisphenol A (TBBPA) with manganese dioxide:
410 Products and pathways. Environ. Sci. Technol. **2009**, *43*, 4480-4486.
411 [38] Fukushima, M.; Fujisawa, N.; Furubayashi, K.; Iwai, H.; Otsuka, K.; Yamamoto, M.; Komai,
412 T.; Kawabe, Y.; Horiya, S. Structural features and Fe(II)-binding capacities of humic acids from
413 reservoir sediments. J. Chem. Eng. Jpn. **2012**, *45*, 452-458.
414 [39] Fukushima, M.; Yamamoto, M.; Komai, T.; Yamamoto, K. Studies of structural alterations of
415 humic acids from conifer bark residue during composting by pyrolysis-gas chromatography/mass
416 spectrometry using tetramethylammonium hydroxide (TMAH-py-GC/MS). J. Anal. Appl. Pyrolysis
417 **2009**, *86*, 200-206.
418

FIGURE CAPTIONS

Figure 1. Influence of FeTPPS concentration on the degradation and debromination of TBBPA at pH 4 (a and b) and 8 (c and d) in the absence and presence of HA. $[TBBPA]_0$ 50 μM, $[KHSO_5]$ 125 μM, [HA] 50 mg L^{-1}, reaction time 30 min.

Figure 2. Influence of FeTPPS concentration on the degradation and debromination of TCBPA at pH 4 (a and b) and 8 (c and d) in the absence and presence of HA. $[TCBPA]_0$ 50 μM, $[KHSO_5]$ 125 μM, [HA] 50 mg L^{-1}, reaction time 30 min.

Figure 3. GC/MS chromatograms for *n*-hexane extracts from the reaction mixtures for TBBPA (a) and TCBPA (b) in the presence of HA. $[TBBPA]_0$ 50 μM, $[KHSO_5]$ 125 μM, [HA] 50 mg L^{-1}.

Figure 4. Mass spectra of the oxidation products shown in Fig. 3. (a) 2HIP-26-DBP (b) coupling product of TBBPA with 26DBP, (c) 2HIP-26-DCP, (d) coupling product of TCBPA with 26DCP.

Figure 5. Kinetics of conversion for TBBPA or TCBPA to 2HIP-26DBP (■) or 2HIP-26DCP (●) (a), and coupling products between TBBPA or TCBPA and 26DBP (■) or 26DCP (●) (b). $[TBBPA]_0$ 50 μM, $[KHSO_5]$ 125 μM, [HA] 50 mg L^{-1}.

Figure 6. (A) Pyrograms of HA fractions from the reaction mixtures as a result of catalytic oxidation with TBBPA (i) and TCBPA (ii), and (B) assigned pyrolysate compounds derived from HA.

Figure 7. Pathways for the production of coupling compounds in the FeTPPS/$KHSO_5$ catalytic system.

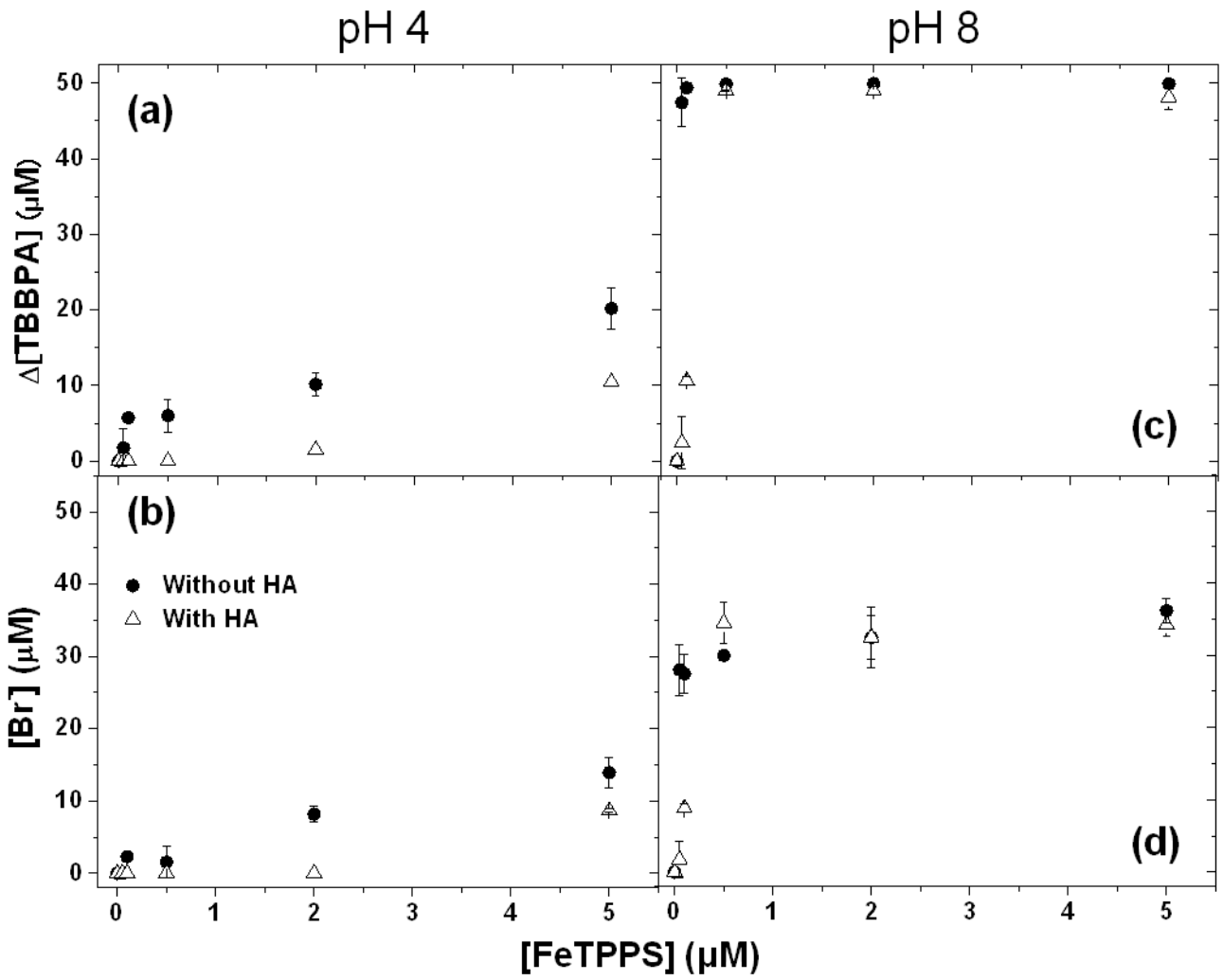

Fig.1 (Mizutani et al.)

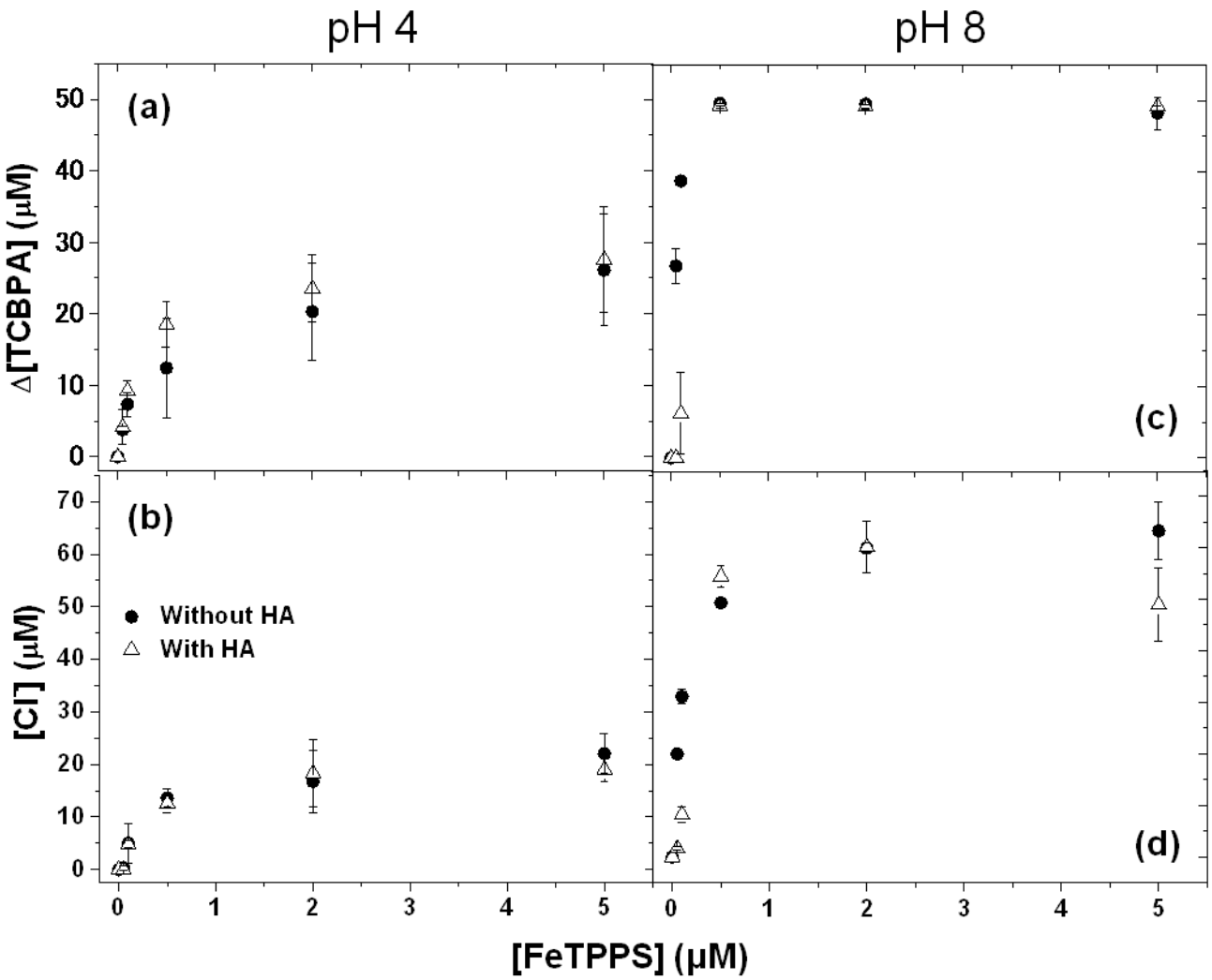

Fig. 2 (Mizutani et al.)

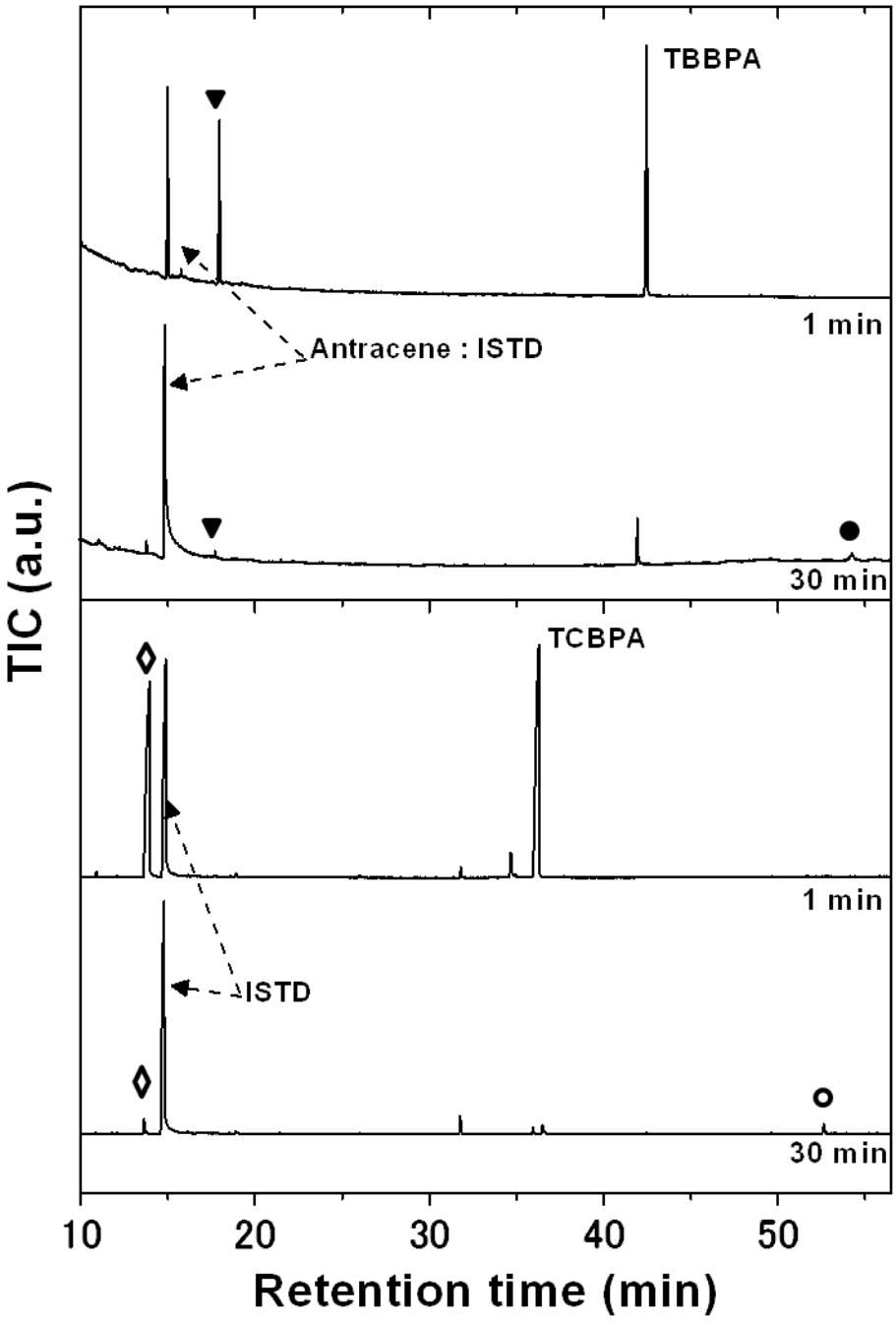

Fig. 3 (Mizutani et al.)

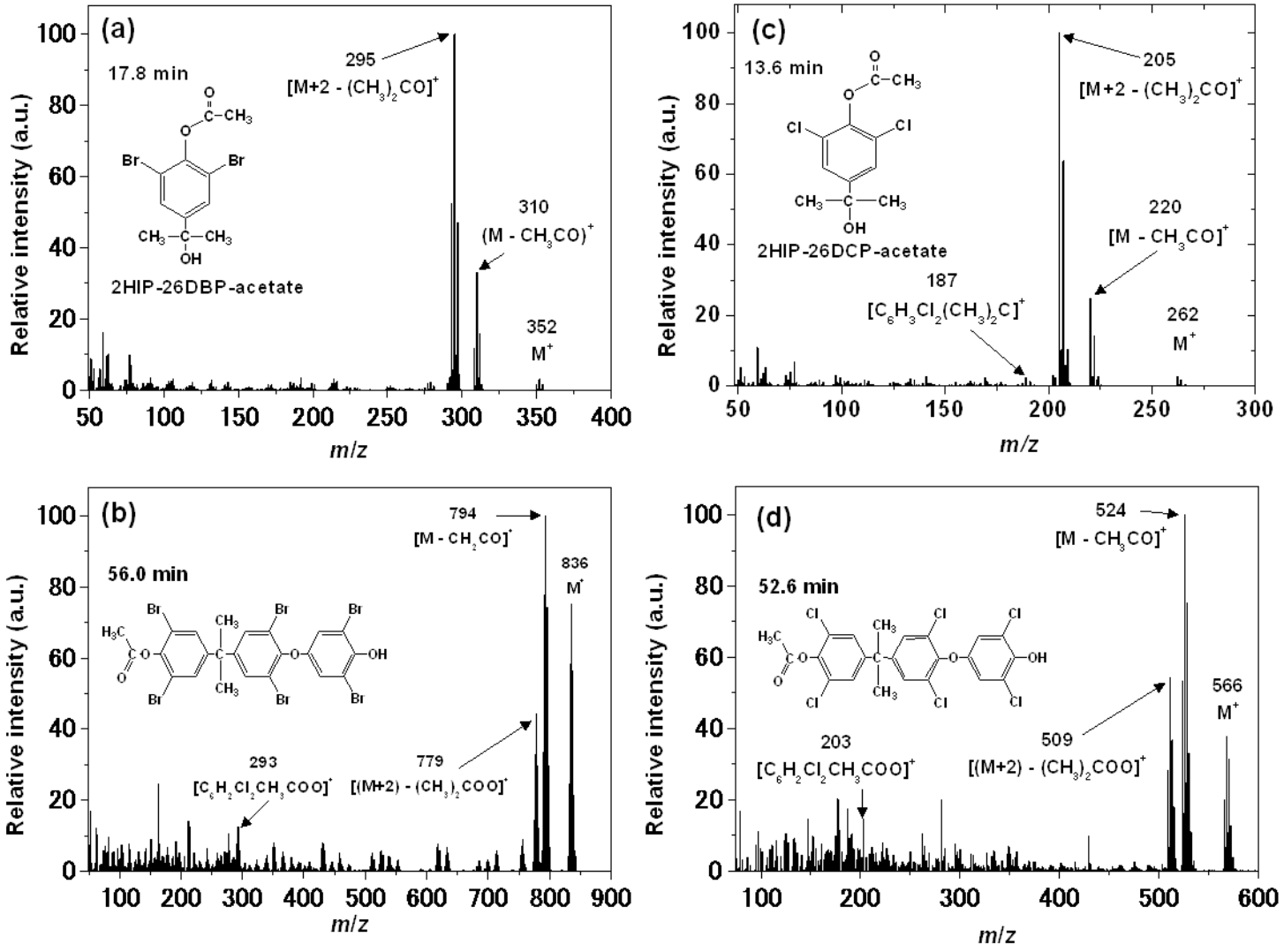

Fig. 4 (Mizutani et al.)

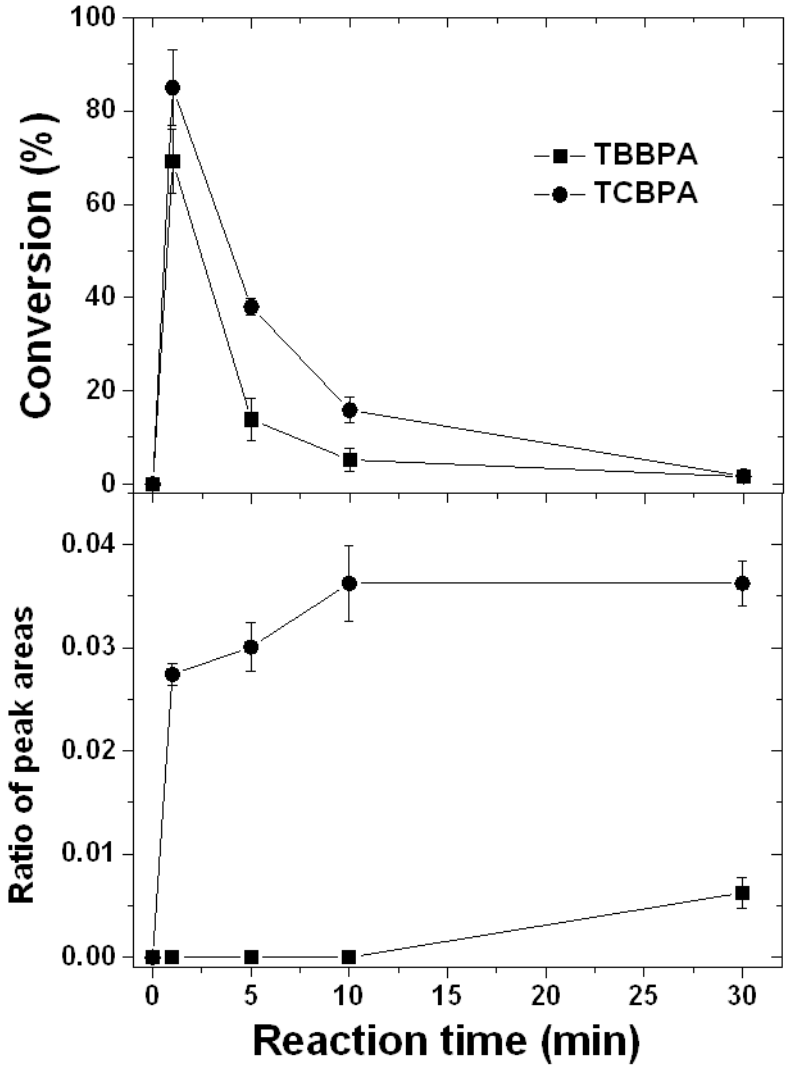

Fig. 5 (Mizutani et al.)

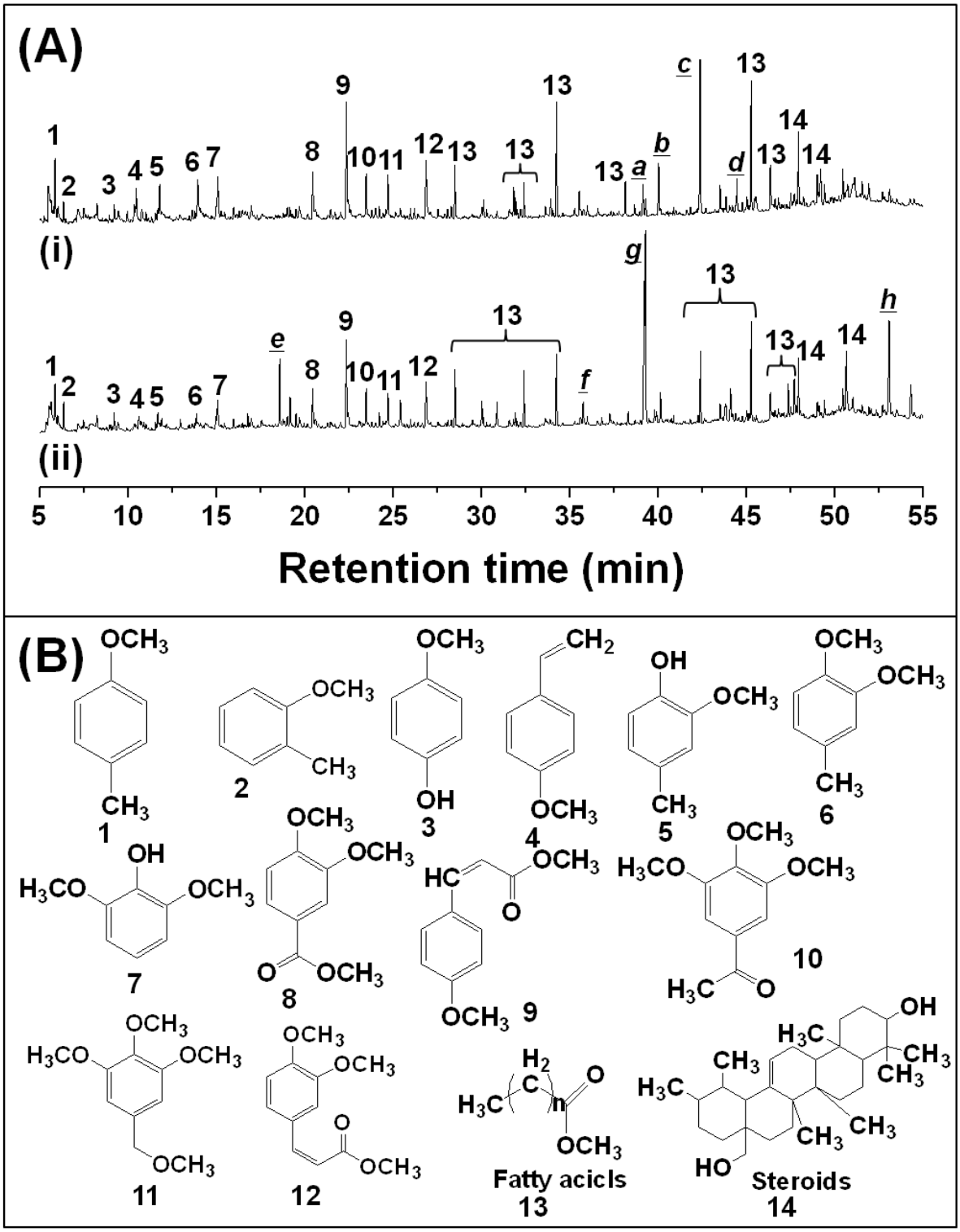

Fig. 6 (Mizutani et al.)

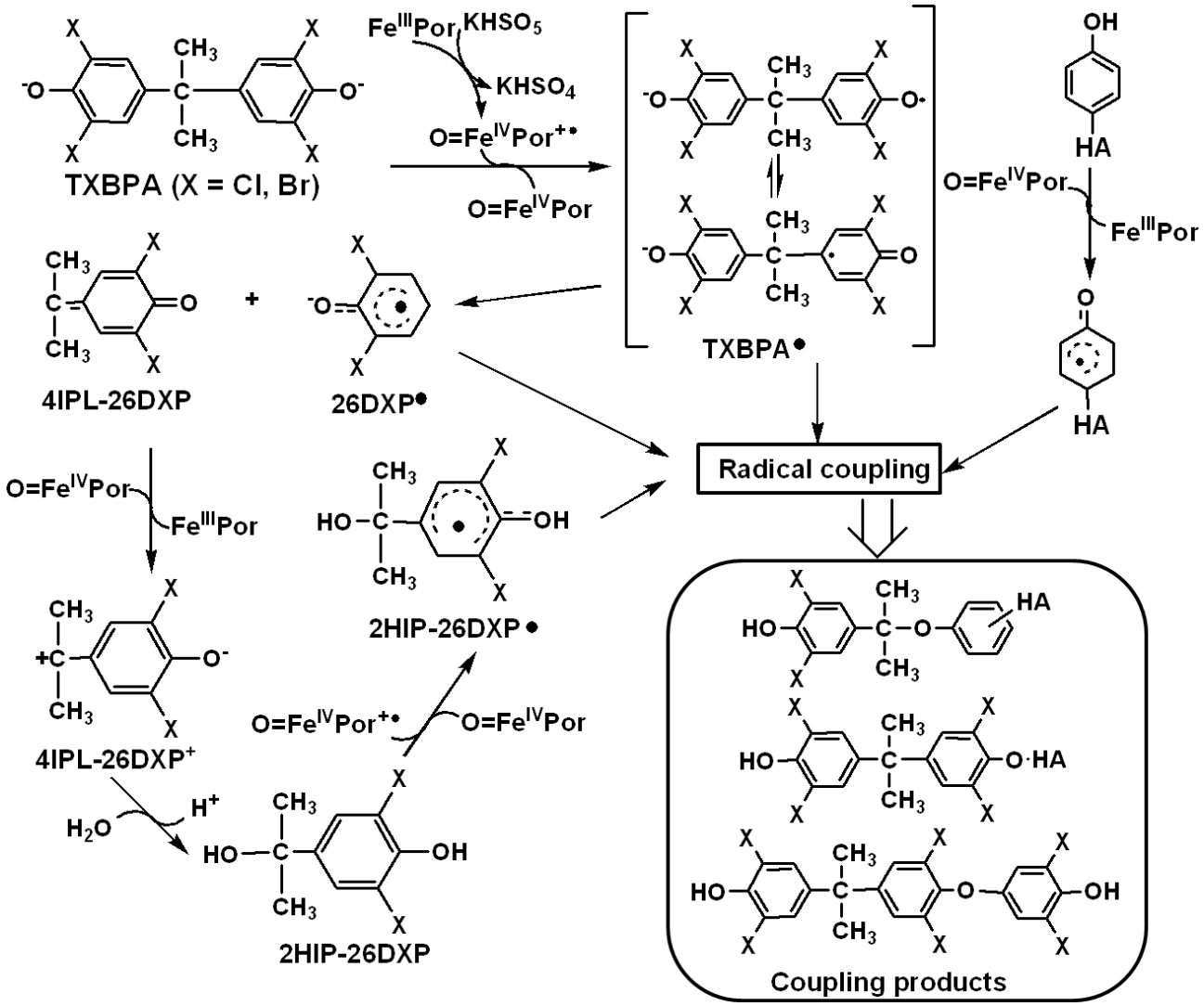

Fig. 7 (Mizutani et al.)

495

Table 1. Estimation of the turnover number for degradation and dehalogenation of TBBPA and TCBPA.

pH	TBBPA or TCBPA degradation		Dehalogenation	
	Without HA	With HA	Without HA	With HA
TBBPA				
4	4.04±0.54 (5)	2.09±0.23 (5)	2.78±0.41 (5)	1.74±0.06 (5)
8	948±64 (0.05)	106±6 (0.1)	560±71 (0.05)	88.1±6.0 (0.1)
TCBPA				
4	24.8±3.3 (0.5)	37.1±6.4 (0.5)	27.2±3.5 (0.5)	25.2±3.5 (0.5)
8	537±48 (0.05)	62.3±2.8 (0.1)	400±14 (0.05)	82.1±14 (0.1)

Values in parenthesis denote the concentration of FeTPPS (μM) for the estimation of TON.

496
497

Table 2. Table 2. Assignments of mass spectra for peaks *a* - *h* from the pyrograms shown in Fig. 6A.

Peaks	m/z [rel. int., fragment identity]	Assigned structures
a	414 [23.0, M^+], 399 [100, $(M - CH_3)^+$], 319 [2.49, $(M - CH_3Br)^+$]	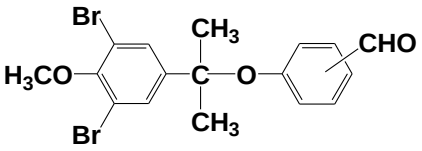
b	492 [53.9, M^+], 489 [100, $(M - CH_3)^+$] 329 [14.2, $(M - CH_3Br_2)^+$]	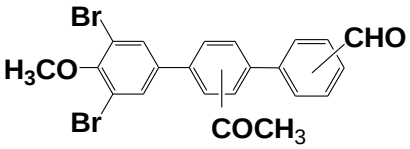
c	572 [30.4, M^+], 557 [100, $(M - CH_3)^+$], 477 [2.86, $(M - CH_3Br)^+$], 397 [5.03, $(M - CH_3Br_2)^+$]	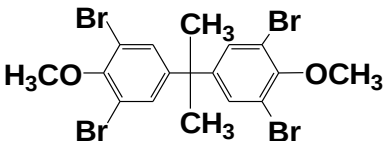
d	504 [53.9, M^+], 498 [100, $(M - CH_3)^+$] 329 [14.2, $(M - CH_3Br_2)^+$]	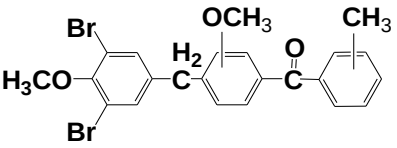
e	216 [100, M^+], 201 [98.9, $(M - CH_3)^+$], 166 [6.62, $(M - CH_3Cl)^+$]	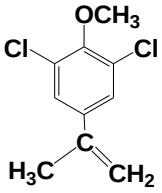
f	357 [26.8, M^+], 342 [100, $(M - CH_3)^+$], 307 [4.20, $(M - CH_3Cl)^+$], 272 [7.55, $(M - CH_3Cl_2)^+$]	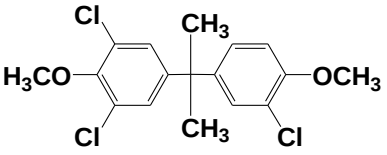
g	392 [22.3, M^+], 377 [81.2, $(M - CH_3)^+$], 342 [2.12, $(M - CH_3Cl)^+$], 307 [3.33, $(M - CH_3Cl_2)^+$]	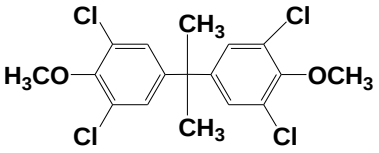
h	554 [78.2, M^+], 539 [100, $(M - CH_3)^+$], 469 [4.07, $(M - CH_3Cl_2)^+$]	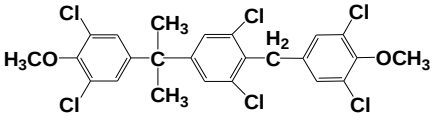

498